

**Bounds on the electromagnetic interactions of excited spin-3/2 leptons**

R. Walsh\* and A. J. Ramalho†

*Instituto de Física, Universidade Federal do Rio de Janeiro, Caixa Postal 68528, Ilha do Fundão, 21945-970 Rio de Janeiro, RJ, Brazil*

(Received 24 March 1999; published 13 September 1999)

We discuss possible deviations from QED produced by a virtual excited spin-3/2 lepton in the reaction  $e^+e^- \rightarrow 2\gamma$ . Data recorded by the OPAL Collaboration at a c.m. energy  $\sqrt{s}=183$  GeV are used to establish bounds on the nonstandard-lepton mass and coupling strengths. [S0556-2821(99)01519-2]

PACS number(s): 12.20.-m, 13.10.+q, 14.60.-z

The success of the standard model in describing the existing phenomenology of the electroweak and strong interactions is rather impressive. Yet few theorists believe the standard model is a fully satisfactory theory of fundamental interactions, since it leaves some important questions unanswered. In view of the shortcomings of the standard model, a host of extended models has been put forward which predict the existence of new particles and interactions. The search for the manifestations of this new physics is a major task to be undertaken by the experimental groups at the present and future colliders. Here we discuss possible effects of an excited spin-3/2 lepton on two-photon production in  $e^+e^-$  collisions. In the literature exotic spin-3/2 particles have appeared in different contexts, with their production rates and decay modes being analyzed in the environments of  $e^+e^-$ ,  $ep$ ,  $e\gamma$ ,  $\gamma\gamma$  and  $pp$  collisions [1–3]. Supersymmetric theories are known to include supermultiplets with spin-3/2 particles. In supergravity gauge theories there are fundamental spin-3/2 fermions, the gravitinos, which can be endowed with typical quantum numbers of the ordinary quarks and leptons. Spin-3/2 fermions are also present in composite models [2,3], in which deviations from the standard model are due to an underlying substructure of quarks and leptons.

Field theories for interacting spin-3/2 particles are known to be nonrenormalizable, violating unitarity at sufficiently high energies [2]. In order to parametrize the effects of a nonstandard spin-3/2 lepton interacting with electrons and photons, we consider two effective interaction Lagrangians

$$\mathcal{L}_{int}^{(1)} = \frac{e}{\Lambda} \bar{\Psi}_\mu^* \gamma_\nu (c_L \psi_L + c_R \psi_R) F^{\mu\nu},$$

$$\mathcal{L}_{int}^{(2)} = \frac{e}{\Lambda^2} \bar{\Psi}_\mu^* \sigma_{\alpha\beta} (c_L \psi_L + c_R \psi_R) \partial^\mu F^{\alpha\beta},$$

where  $\Psi_\mu$  is a Rarita-Schwinger vector-spinor field representing the excited spin-3/2 lepton,  $\psi_{L,R}$  are definite-helicity Dirac spinor fields corresponding to the electrons, and  $F^{\mu\nu}$  is the electromagnetic field strength.  $\Lambda$  is a characteristic energy scale around which effects of the new physics would become manifest. Both Lagrangians above are gauge invariant. It is important to point out that, to avoid running into conflict with  $(g-2)$  measurements of electrons and muons,

one must couple the spin-3/2 lepton exclusively to left-handed or right-handed ordinary leptons [3].

The process  $e^+e^- \rightarrow 2\gamma$  is a very convenient tool to search for physics beyond the standard model. The total and differential cross sections can be measured with precision at the CERN  $e^+e^-$  collider LEP [4,5]. We used data taken by the OPAL Collaboration [4] at a center-of-mass energy  $\sqrt{s}=183$  GeV and total integrated luminosity of  $56.2 \text{ pb}^{-1}$  to obtain lower bounds on the mass scale  $\Lambda$ , as well as on the spin-3/2 excited-lepton mass  $M_{3/2}$  and coupling strengths  $c_{L,R}$ . The calculation of the differential cross section for two-photon production was performed at tree level, taking into account the nonstandard couplings specified by  $\mathcal{L}_{int}^{(1)}$  and  $\mathcal{L}_{int}^{(2)}$ . The resulting expressions are given by

$$\frac{d\sigma^{(i)}}{d\Omega} = \left( \frac{d\sigma}{d\Omega} \right)_{QED} + \frac{\alpha^2}{16s} [F_+^{(i)}(c_L, c_R, x, y, s/\Lambda^2) + F_-^{(i)}(c_L, c_R, x, y, s/\Lambda^2)], \quad i=1,2,$$

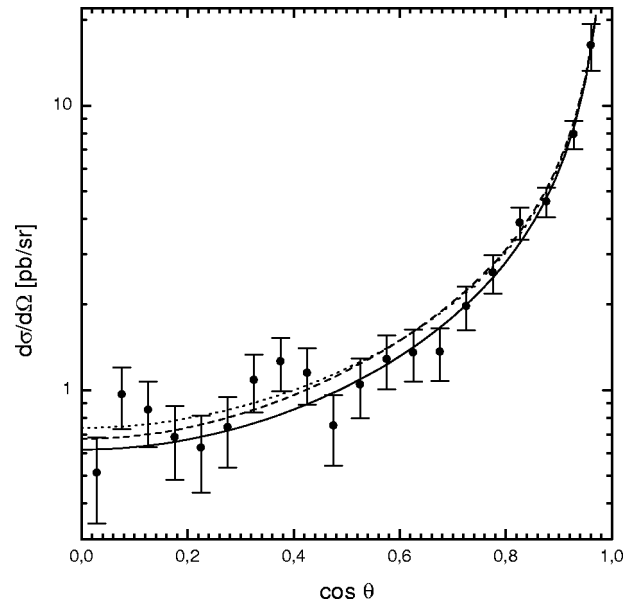


FIG. 1. Angular distribution at  $\sqrt{s}=183$  GeV. The solid curve represents the QED prediction, whereas the dashed (dotted) curve shows the total angular spectrum in the presence of the nonstandard interaction  $\mathcal{L}_{int}^{(1)}$  ( $\mathcal{L}_{int}^{(2)}$ ) for an input mass  $M_{3/2}=125$  GeV (142 GeV). OPAL data are also shown for comparison.

\*Email address: walsh@if.ufrj.br

†Email address: ramalho@if.ufrj.br

TABLE I. Coefficients  $a_n(y)$  for the polynomials of the corrections  $F_{\pm}^{(i)}$ .

	$a_8$	$a_7$	$a_6$	$a_5$	$a_4$	$a_3$	$a_2$	$a_1$	$a_0$
$A_+^{(1)}$	0	0	-1	$2y+4$	$-10y^2+2y$	$-32y^2-28y$	$8y^3+48y^2$	$-16y^3-32y^2$	$80y^3+26y^2$
$A_-^{(1)}$	0	0	-1	$2y+4$	$-10y^2-14y$	$36y$	$-8y^3-48y^2$	$16y^3+64y^2$	$-80y^3-6y^2$
$B_+^{(1)}$	0	0	0	0	$3y+13$	0	$-4y^2-8y$	0	$40y^2+5y$
$B_-^{(1)}$	0	0	0	0	$3y+5$	0	$4y^2+8y$	0	$-40y^2-11y$
$C^{(1)}$	0	0	0	0	-2	$y+8$	$-11y-12$	$7y+8$	$3y-2$
$D^{(1)}$	0	0	0	0	-1	$-3y-2$	$y$	$3y+2$	$-y+1$
$A_+^{(2)}$	-1	6	$-4y-14$	14	$12y^2+60y$	$-120y^2-160y$	$72y^3+288y^2$	$-144y^3-264y^2$	$72y^3+84y^2$
$A_-^{(2)}$	1	-6	$20y+14$	$-96y-14$	$84y^2+180y$	$-264y^2-160y$	$72y^3+288y^2$	$-144y^3-120y^2$	$72y^3+12y^2$
$B^{(2)}$	0	0	-1	0	$-6y+3$	0	$-9y^2-3$	0	$9y^2+6y$
$C^{(2)}$	0	0	0	-1	3	$-2y-2$	$6y-2$	$-6y+3$	$2y-1$
$D^{(2)}$	0	0	0	0	-2	$-4y-4$	$-4y$	$4y+4$	$4y+2$

where  $(d\sigma/d\Omega)_{QED} = (\alpha^2/s)(1+x^2)/(1-x^2)$  is the photon angular distribution expected from QED,  $x \equiv \cos \theta$ ,  $y \equiv 2M_{3/2}^2/s$ , and the nonstandard corrections read

$$F_{\pm}^{(1)} = \frac{s^2}{\Lambda^4} \frac{(c_R^2 + c_L^2)^2}{72y^2(1-y-x)} \left[ \frac{A_{\pm}^{(1)}(x,y)}{(1-y-x)} + \frac{2yB_{\pm}^{(1)}(x,y)}{(1+y+x)} \right] + \frac{s}{\Lambda^2} \frac{(c_R^2 + c_L^2)}{6y(1-x)} \left[ \frac{C^{(1)}(x,y)}{(1-y-x)} + \frac{D^{(1)}(x,y)}{(1+y+x)} \right] + (x \rightarrow -x),$$

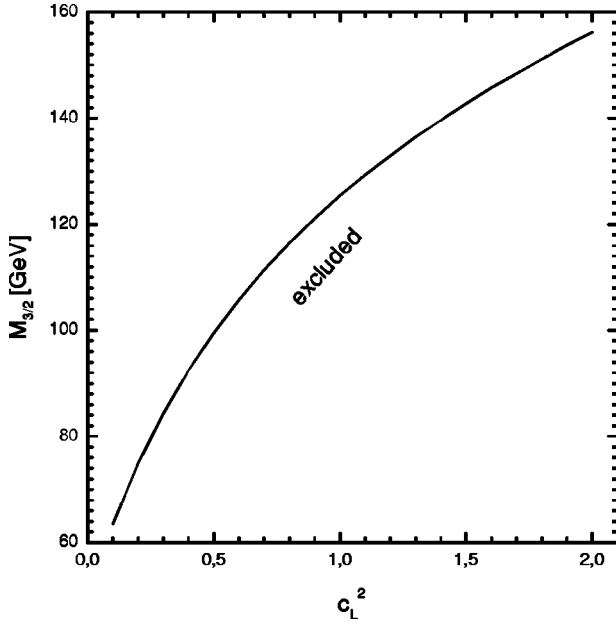


FIG. 2. 95% C.L. lower bound on the spin-3/2 lepton mass  $M_{3/2}$  as a function of  $c_L^2$  for interaction  $\mathcal{L}_{int}^{(1)}$  and c.m. energy  $\sqrt{s} = 183$  GeV.

$$F_{\pm}^{(2)} = \frac{s^4}{\Lambda^8} \frac{(c_R^2 + c_L^2)^2}{288y^2(1-y-x)} \left[ \frac{A_{\pm}^{(2)}(x,y)}{(1-y-x)} + \frac{4yB^{(2)}(x,y)}{(1+y+x)} \right] + \frac{s^2}{\Lambda^4} \frac{c_R c_L}{3y(1-x)} \left[ \frac{C^{(2)}(x,y)}{(1-y-x)} + \frac{D^{(2)}(x,y)}{(1+y+x)} \right] + (x \rightarrow -x),$$

where  $A_{\pm}^{(i)}$ ,  $B_{\pm}^{(i)}$ ,  $B^{(2)}$ ,  $C^{(i)}$  and  $D^{(i)}$ ,  $i=1,2$ , are polynomials written in the form  $\sum_n a_n(y)x^n$ , with the  $y$ -dependent coefficients  $a_n(y)$  given in Table I. Figure 1 shows the angular distributions  $d\sigma^{(i)}/d\Omega$  at  $\sqrt{s} = 183$  GeV, along with the cor-

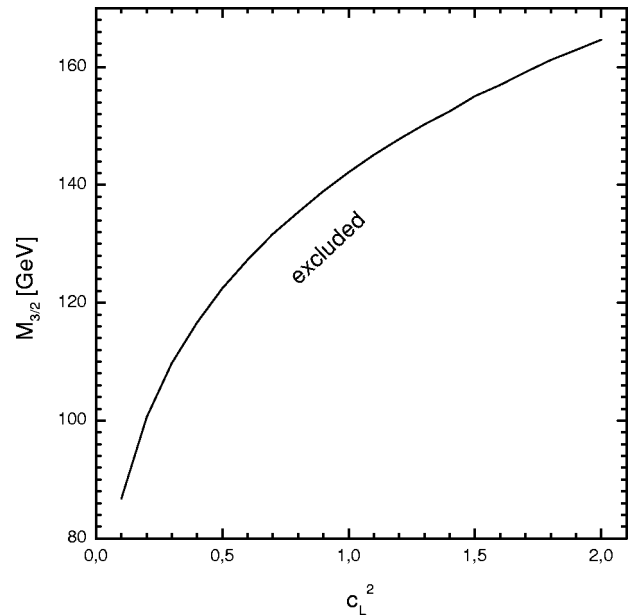


FIG. 3. Same as Fig. 2 but for interaction  $\mathcal{L}_{int}^{(2)}$ .

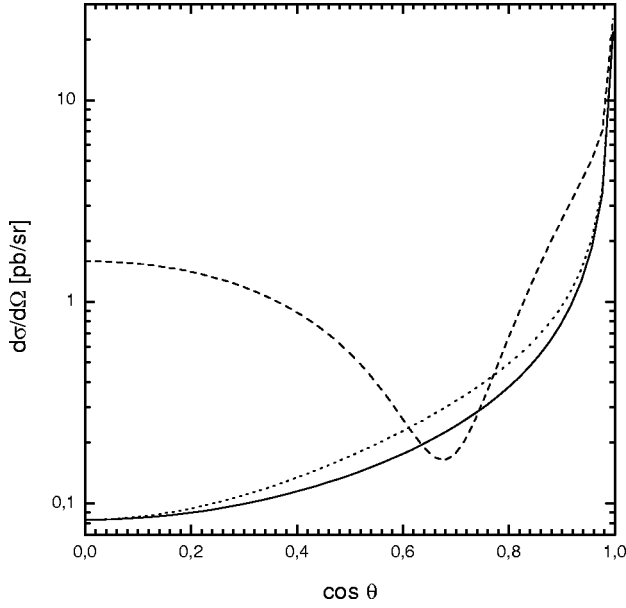


FIG. 4. Angular distribution at  $\sqrt{s}=500$  GeV. The solid line represents the QED prediction, whereas the dashed (dotted) curve shows the total angular spectrum in the presence of the nonstandard interaction  $\mathcal{L}_{int}^{(1)}$ , for an input mass  $M_{3/2}=125$  GeV (250 GeV).

responding prediction for QED and OPAL experimental data. In line with OPAL experimental procedure, we consider the event angle  $\theta$  defined so that  $\cos \theta$  is positive, since the two photons are identical, and an experimental cut  $\cos \theta < 0.97$ . The compositeness scale  $\Lambda$  was taken to be equal to the exotic-lepton mass, with numerical values consistent with the 95% confidence level lower bounds that we derived for each interaction, as discussed in the following.

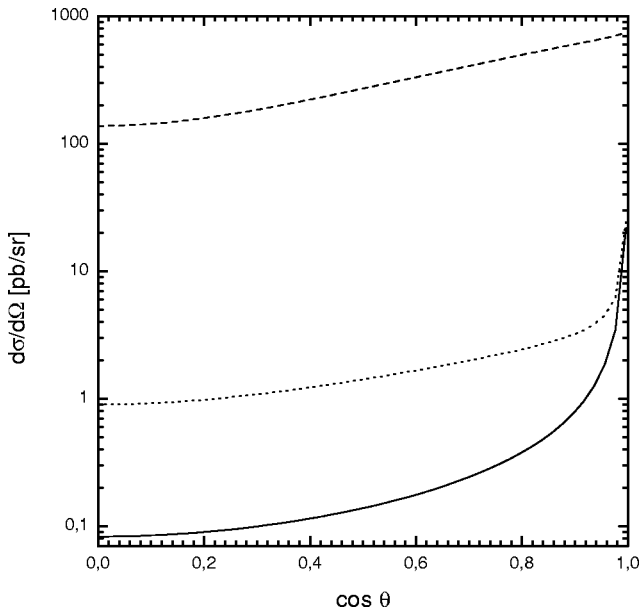


FIG. 5. Angular distribution at  $\sqrt{s}=500$  GeV. The solid line represents the QED prediction, whereas the dashed (dotted) curve shows the total angular spectrum in the presence of the nonstandard interaction  $\mathcal{L}_{int}^{(2)}$ , for an input mass  $M_{3/2}=142$  GeV (250 GeV).

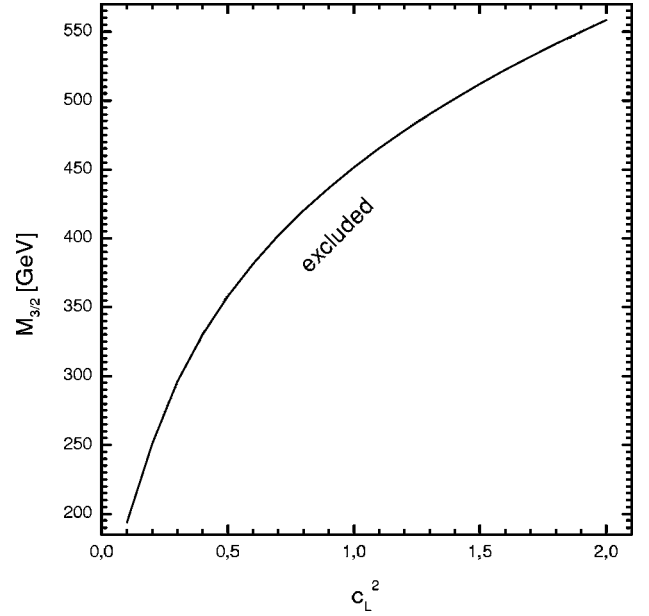


FIG. 6. Same as Fig. 2 but for a NLC energy  $\sqrt{s}=500$  GeV.

We derived lower bounds on the exotic-lepton mass and couplings by a  $\chi^2$  fit, defining

$$\chi^2(i) = \sum_k \left( \frac{\sigma_k^{(i)} - \sigma_k^{exp}}{\Delta \sigma_k} \right)^2, \quad i=1,2,$$

where  $\sigma_k^{(i)} \equiv (d\sigma^{(i)}/d\Omega)_k$  denotes the theoretical value of the angular distribution for the  $k$ th bin,  $\sigma_k^{exp} \equiv (d\sigma^{exp}/d\Omega)_k$  denotes the corresponding experimental value measured by the OPAL Collaboration and  $\Delta \sigma_k$  its associated experimental error for the  $k$ th bin. Bounds on  $M_{3/2}$  were computed for fixed values of the couplings. These lower bounds at the 95% confidence level correspond to an increase  $\Delta \chi^2 = 3.84$  with

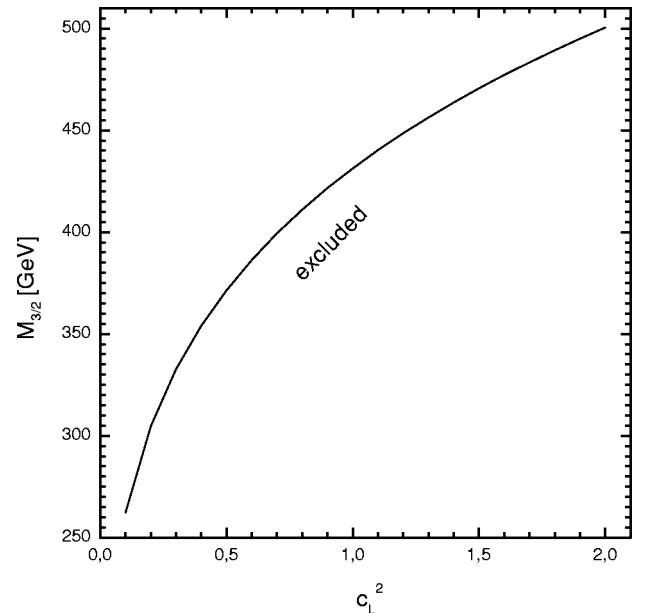


FIG. 7. Same as Fig. 3 but for a NLC energy  $\sqrt{s}=500$  GeV.

respect to the minimum. For  $c_L^2=1$  and  $c_R^2=0$ , for instance, the lower limits are  $M_{3/2}>125$  GeV and  $M_{3/2}>142$  GeV for interactions  $\mathcal{L}_{int}^{(1)}$  and  $\mathcal{L}_{int}^{(2)}$  respectively. Figures 2 and 3 show the 95% C.L. bounds on  $M_{3/2}$  as functions of  $c_L^2$ , with  $c_R^2=0$ . The lower limits are the same if one interchanges  $c_L$  and  $c_R$ .

The next generation of linear  $e^+e^-$  colliders (NLC) will give important contributions to the search of nonstandard physics. Angular distributions for a 500 GeV NLC are shown in Figs. 4 and 5, considering interactions  $\mathcal{L}_{int}^{(1)}$  and  $\mathcal{L}_{int}^{(2)}$  respectively, and assuming an input mass  $M_{3/2}=250$  GeV or the lower bound which we obtained from the OPAL data. We considered a cut in the polar angle  $\theta$  such that  $5^\circ<\theta<175^\circ$ . As expected, cross sections grow faster with energy in the presence of the nonstandard interactions under discussion, the more so in the case of  $\mathcal{L}_{int}^{(2)}$ , which contains a higher-dimensional operator. In order to estimate lower bounds in this case, we defined  $\chi^2$  functions

$$\chi^2(i) = \sum_k \left( \frac{N(i)_k - N_k^{SM}}{\Delta N_k^{SM}} \right)^2, \quad i=1,2,$$

where  $N(i)_k$  stands for the number of events in the  $k$ th bin in the presence of the nonstandard electromagnetic interactions,  $N_k^{SM}$  is the number of events predicted by the standard model for the same bin, and  $\Delta N_k^{SM} = \sqrt{N_k^{SM} + (N_k^{SM} \delta)^2}$  is the corresponding error, in which the Poisson-distributed statistical error is combined in quadrature with the systematic error. We considered a conservative integrated luminosity of  $10 \text{ fb}^{-1}$  and a typical systematic error  $\delta=2\%$  for a measurement in a 500 GeV NLC. The results of this  $\chi^2$  analysis are displayed in Figs. 6 and 7. Clearly, the lower bounds can be considerably improved by the experiments in the future  $e^+e^-$  colliders.

We thank K. Sachs from OPAL for the data used in this paper. This work was partly supported by CNPq and FINEP.

- 
- [1] J. Leite Lopes, J.A. Martins Simões, and D. Spehler, Phys. Rev. D **23**, 797 (1981); **25**, 1854 (1982); D. Spehler, O.J.P. Éboli, G.C. Marques, S.F. Novaes, and A.A. Natale, *ibid.* **36**, 1358 (1987); B. Moussallam and V. Soni, *ibid.* **39**, 1883 (1989); F.M.L. Almeida, Jr., J.A. Martins Simões, and A.J. Ramalho, Nucl. Phys. **B397**, 502 (1993); J.C. Montero and V. Pleitz, Phys. Lett. B **321**, 267 (1994); F.M.L. Almeida, Jr., J.H. Lopes, J.A. Martins Simões, and A.J. Ramalho, Phys. Rev. D **53**, 3555 (1996); O.J.P. Éboli, E.M. Gregores, J.C. Montero, S.F. Novaes, and D. Spehler, *ibid.* **53**, 1253 (1996); D.A. Dicus, S. Gibbons, and S. Nandi, hep-ph/9806312 1998.
- [2] J. Leite Lopes, J.A. Martins Simões, and D. Spehler, Phys. Lett. **94B**, 367 (1980); C.J.C. Burges and Howard J. Schnitzer, Nucl. Phys. **B228**, 464 (1983); K. Senba and M. Tanimoto, Phys. Lett. **152B**, 363 (1984).
- [3] J. Kühn and P. Zerwas, Phys. Lett. **147B**, 189 (1984); S.R. Choudhury, R.G. Ellis, and G.C. Joshi, Phys. Rev. D **31**, 2390 (1985).
- [4] OPAL Collaboration, K. Ackerstaff *et al.*, Phys. Lett. B **438**, 379 (1998).
- [5] ALEPH Collaboration, R. Barate *et al.*, Phys. Lett. B **429**, 201 (1998); DELPHI Collaboration, P. Abreu *et al.*, *ibid.* **433**, 429 (1998).